JOURNAL OF MATERIALS SCIENCE 31 (1996) 2385–2392

Experimental evaluation of residual stresses in single fibre composites by means of the fragmentation test

M. DETASSIS, A. PEGORETTI*, C. MIGLIARESI
Department of Materials Engineering, University of Trento, 38050 Trento, Italy
H. D. WAGNER
Department of Materials & Interfaces, The Weizmann Institute of Science, 76100 Rehovot, Israel

The residual stresses in both thermosetting and thermoplastic single-fibre composites have been experimentally evaluated by means of an original technique based on the continuous monitoring of the fragmentation test performed at various temperatures. The difference between the strain at the break of a single fibre in air and one embedded in a polymeric matrix has been measured as a function of temperature. By considering the compressive fibre modulus this strain difference has been converted into fibre compressive stresses related to the matrix thermal shrinkage after curing of the samples. In fact, as the test temperature increased, the thermal compressive stresses decreased until a zero value was obtained, corresponding to a so called "stress free temperature", equal to the curing temperature for amorphous thermosetting matrix composites or equal to the matrix melting temperature for semicrystalline-thermoplastic matrix composites. The experimental results have been compared with data obtained from a theoretical model and a good agreement was found especially if the temperature dependence of the matrix Young's modulus and matrix thermal expansion coefficient are accounted for in the computation.

1. Introduction

Processing methods currently used both for thermosetting and thermoplastic matrix composites involve thermal treatments at elevated temperatures. Generally, the thermal expansion properties of the fibres and the matrix are very different and so residual thermal stresses will always build up after cooling of the composite material. Over the years, various works have focused on the issue of the residual stresses in composite materials [1–5], nevertheless the study of the effect of these stresses in microcomposites is a relatively new task [6–8].

In general in a composite material the fibre is under compression, both in axial and radial directions, with higher stress values at smaller fibre volume fractions. Such stresses are therefore especially large in single fibre composites, which are the typical microcomposites used in the interfacial shear strength measurement by means of the fragmentation test [8]. The residual stresses exerted on the fibre in the axial direction may promote fibre breaks under compression (such as in carbon/thermoplastic composites) or induce fibre buckling as reported for carbon and glass/thermosetting composites [8–13]. In addition, pre-tension is often induced in the fibre during the sample preparation, which involves alignment of the fibre in a mould and fixing with adhesives. In the radial direction residual stresses may exert frictional forces at the interface and therefore affect the interfacial shear strength [7, 14, 15].

As a result of the above considerations, residual stresses may have a great influence on the mechanical behaviour of microcomposites and therefore they should be accounted for whenever the actual fibre stresses or the actual interfacial stresses are under investigation.

The aim of this work is to present a simple technique, based on the fibre fragmentation phenomenon, by which it is possible to measure the fibre residual stresses in both thermosetting and thermoplastic matrix microcomposites.

2. Theory

2.1. Fragmentation test

The fragmentation method, proposed by Fraser *et al.* [16], is widely used for measuring the interfacial shear strength in polymeric matrix composites. In the fragmentation test a sample, consisting of a single fibre embedded longitudinally in a matrix, is put under

*Author to whom correspondence should be addressed

0022–2461

tension. As the applied strain increases, the fibre breaks at any point where the stress equals the fibre strength. A continuous increase of the strain induces further breaks until the fragments are too short to allow the transfer of stress equal to or greater than the fibre tensile strength. Such a critical point is defined as the saturation of the fragmentation process. The mean length of the fragments at saturation is related to the interfacial shear strength (τ) by the Kelly–Tyson relationship [17]:

$$\tau = \frac{d\sigma_b(L_c)}{2L_c} \quad (1)$$

where d is the fibre diameter, L_c the critical length which is related to the mean fragments length at saturation $\bar{L}_s$ (according to Ohsawa *et al.* [18] we assumed $L_c = 4/3\,\bar{L}_s$) and $\sigma_b(L_c)$ is the mean fibre strength at the fibre critical length. Because critical lengths are usually in the range 0.2–2 mm, $\sigma_b(L_c)$ cannot be directly measured. The fibre strength generally obeys a Weibull distribution [19] and therefore $\sigma_b(L_c)$ can be computed as:

$$\sigma_b(L_c) = \sigma_o L_c - \frac{1}{m}\Gamma\left(1 + \frac{1}{m}\right) \quad (2)$$

where σ_o is the Weibull scale parameter (i.e. the strength at which the cumulative probability of failure of a fibre 1 mm in length is about 63%), m is the Weibull shape parameter, which is inversely related to the spread of the strength distribution, and Γ is the Gamma function. Also, the length L_c used in this equation is dimensionless [11]. Two techniques are currently used to obtain the Weibull parameters of the fibre strength: the single fibre test (SFT) [20, 21] and the continuously monitored single filament composite test (CMSFCT) [21, 22]. In the former a large number of tensile tests (usually more than 20) are carried out in air on single fibres in order to get the mean value of fibre strength at a certain gauge length. The same procedure is repeated at various gauge (usually 4 in a range from 5–200 mm) and finally Weibull parameters are obtained by an extrapolation based on Equation 2 rearranged as follows,

$$\ln(\sigma_b) = -\frac{1}{m}\ln(L) + \ln\left[\sigma_o\Gamma\left(1 + \frac{1}{m}\right)\right] \quad (3)$$

The second method consists in the simultaneous monitoring of the fibre stress (σ) and the mean fragment length ($\bar{L}$) in a sample during a fragmentation test. In fact as reported by Yavin *et al.* [21] the interpolation of the data according to the following equation:

$$\ln(\bar{L}) = -m\ln(\sigma) + m\ln\left[\sigma_o\Gamma\left(1 + \frac{1}{m}\right)\right] \quad (4)$$

gives the *in-situ* Weibull parameters for the fibre strength. The fibre stress σ is usually obtained from the stress σ_c applied to the sample and the fibre (E_f) and matrix (E_m) tensile moduli by the following relationship: $\sigma = \sigma_c E_f/E_m$.

CMSFCT is less time consuming than SFT and sometimes seems to provide more accurate data by overcoming the problem of the "wide" extrapolation necessary in the SFT method. Nevertheless the CMSFCT has an evident shortcoming. Residual (pretension or thermal) stresses almost always exist in the fibre and therefore they should be accounted for in the evaluation of the fibre strength from experimental data.

2.2. Evaluation of residual stresses through the fragmentation test

The approach consists in focusing on the effect of residual strain on the evolution of the fragmentation process. In fact, as experimentally observed, a pre-existing compressive strain in the fibre causes the fragmentation process to be delayed (that is, the process starts at apparently higher applied stresses). Conversely, a pre-existing tensile strain in the fibre causes the fragmentation process to occur sooner [23] (that is, the process starts at apparently lower applied stresses), with respect to a hypothetical stress-free situation. This is what we call the "strain shift" effect of residual stresses in the fragmentation test.

An evaluation of this strain shift effect has been already obtained by Vautey *et al.* [24] from the difference between the strain at which the fragmentation starts (first fibre break) in carbon/PET samples and the strain at break of the same fibre in air measured by the standard SFT. However, because of the fibre strength distribution, the strain associated with the first break is rather variable, being associated to a gross fibre defect. Therefore, to place confidence on that value, a large number of tests should be performed. Yavin *et al.* [21], Scherf and Wagner [23], and Waterbury and Drzal [25] measured the mean fragment length, L, as a function of the applied stress, σ, during the whole fragmentation process and they plotted these values in a $\ln(\sigma)$ versus $\ln(L)$ graph to compare the fragmentation trend with the analogous obtained from the standard single fibre tests. The strain shift of the two curves was explained as a fibre pre-tensioning.

Our method (see Fig. 1) is based on the measure of the strain difference between the applied strain, ε^*, which induces an arbitrary number of breaks along a fibre embedded in a matrix (and consequently a mean fragment length equal to L^*) and the mean strain at break, ε_b, of a single fibre of length $2L^*$ tested in air (which produces a mean fragment length equal to L^*). In particular, for ε^* we considered the strain necessary to obtain 5 breaks along a 25 mm long fibre embedded in a matrix (and therefore we obtained $L^* = 4.17$ mm), and consequently for ε_b we considered the strain at break of a single fibre in air, whose length is equal to 8.34 mm. Therefore the residual strain in the fibre, ε_r, is given by:

$$\varepsilon_r = \varepsilon^* - \varepsilon_b \quad (5)$$

and the residual stress,

$$\sigma_r = E_f\varepsilon_r \quad (6)$$

Note that the number of fibre breaks has been limited to 5 because, as will be shown later, the spread in the

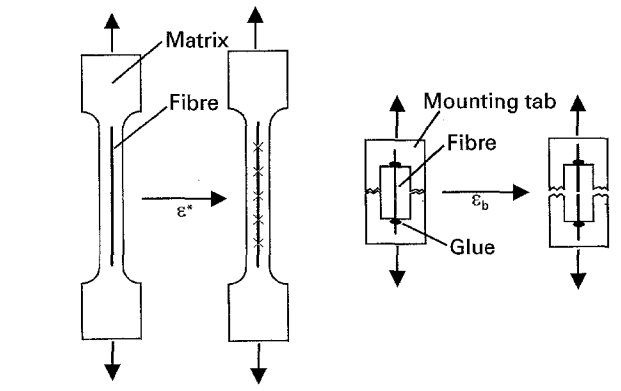

Figure 1 Schematic illustration of the tensile testing procedure for a single fibre embedded in a matrix (a) or a single fibre in air (b).

measured ε* values does not strongly decrease by taking a higher number of fibre breaks.

The method is affected by some approximations, these are as follows:

(i) the strength distribution of the fibre fragments is a truncated Weibull distribution, whereas the strength distribution of independently tested fibres of the same length is an untruncated Weibull distribution. In practice, this tends to give breaking strains that are slightly higher than the actual ones;

(ii) the sample strain may not be exactly equal to the fibre strain, but as long as the matrix is stiff and the interface is relatively strong, this is a good approximation.

2.3. Theoretical estimation of thermal residual stresses

If pre-tension stresses are absent or reasonably negligible, the residual stresses in the fibre should only be thermal. The validity of the proposed method was tested by comparing the measured residual stresses with those evaluated by theoretical models. In this work the approximate model presented by Tsai and Hahn [26] for the built in stresses was used. This approach which is based on the classical "shrink-fit" elastic theory for concentric cylinders (for a review, see references [8] and [12]) yields the following expression for the fibre residual thermal stress, σ_{th} in the axial direction:

$$\sigma_{th} = (\alpha_m - \alpha_f)(T - T_{ref}) \frac{E_f}{1 + \left(\frac{\phi_f}{\phi_m}\right)\left(\frac{E_f}{E_m}\right)} \quad (7)$$

where α and E are the coefficient of thermal expansion and the Young's modulus respectively, ϕ is the volume fraction, the subscripts m and f refer to the matrix and the fibre respectively, T is the test temperature, and T_{ref} is the stress free temperature.

3. Experimental procedure

3.1. Materials

The fibre used in this work was a carbon fibre Besfight HTA–7–3000 from Toho Rayon Co. The thermosetting matrix was an epoxy resin diglycidyl ether of bisphenol-A (Eposir 7120, SIR S.p.A.), cured with 24 phr by weight of isophorone diamine (ID 01784, SIR S.p.A.). The thermoplastic matrix was a nylon-6 film (SNIA S.p.A.) with a thickness equal to 100 μm.

The microcomposites were prepared according to the following procedure: Thermosetting microcomposites: (i) single fibres were placed in dogbone shaped cavities (4×1 mm^2 in cross-section and 25 mm guage length) of a plasticine mould put on a polyethylene sheet; (ii) fibres were fixed using a quick-setting adhesive and the mould was vacuum degassed; (iii) the defoamed catalysed resin was poured into the mould; (iv) the assembly was cured for 2 h at 60 °C; v) the samples were removed from the plasticine mould, postcured at 140 °C for 2 h, cooled overnight to room temperature, and surface polished with sand paper.

Thermoplastic microcomposites: (i) 15 parallel fibres were placed between two nylon-6 films and fixed using an adhesive tape; (ii) the assembly was placed in a mould consisting of two flat aluminium plates covered with a mould releasing agent (iii) the mould was put in a oven under vacuum at a temperature of 280 °C and at a pressure of 7 KPa for 30 min; (iv) after cooling overnight, samples were obtained by cutting strips ($50 \times 55 \times 0.190$ mm^3) containing one single fibre each, longitudinally aligned in the centreline.

3.2. Fibre properties

Scanning electron microscopy (SEM) observations revealed that the carbon fibres had a circular cross-section, whose diameter was measured by an optical microscope and an image analyser system [15]. From about 50 measurements a mean diameter equal to 7.0 ± 0.7 μm was obtained. The fibre strength was evaluated at room temperature by the single fibre test, according to the ASTM D 3379–75 standard, by using an Instron 4502 tensile tester a cross-head speed of 0.2 mm min^{-1}. At least 20 specimens were tested at several gauge lengths (5, 10, 15, 20 mm) to obtain the mean fibre strength. The Weibull parameters shown in Table I were obtained from these data by using Equation 3. By taking the system compliance into account, as recommended by the ASTM standard D 3379–75, the resulting fibre tensile modulus was found to be equal to 246 ± 26 GPa.

TABLE I Thermomechanical properties for carbon fibre, epoxy, and nylon-6

	Carbon fibre	Epoxy	Nylon-6
Longitudinal tensile modulus (GPa)	246 (E_f)	2.98 (E_m)	2.00 (E_m)
Longitudinal coefficient of thermal expansion (10^{-6} K^{-1})	−1* (α_f)	52 (α_m)	104 (α_m)
Weibull scale parameter (MPa)	5949 (σ_0)	–	–
Weibull shape parameter	4.8 (m)	–	–

(*) From technical data sheet.

3.3. Matrix properties

Differential Scanning Calorimetry (DSC) measurements were performed by using a Mettler DSC 30 apparatus. Scans ranged from −50 to +250 °C, at a heating rate of 10 °C min^{-1}, under a nitrogen flux of 10 ml min^{-1}. The epoxy resin showed a glass transition temperature (T_g) of 152 °C, whereas moulded nylon-6 exhibited a T_g of 53.5 °C, a melting temperature of 226 °C and a crystallinity content equal to 29.3% by weight. The tensile modulus data reported in Table I were evaluated at room temperature using the Instron machine on 5 specimens tested at a strain rate equal to 0.008 min^{-1}.

Dynamic–mechanical properties were measured in the tensile mode under nitrogen by a dynamic mechanical thermal analyser (DMTA, model MKII, by Polymer Laboratories Ltd, Loughborough, UK). Both epoxy and nylon-6 matrices were tested at a frequency of 5 Hz, in the temperature range 0–200 °C, at a heating rate of 1 °C min^{-1}. From DMTA measurements, the thermal expansion coefficients of the matrices were evaluated from the slope of the displacement curve as a function of temperature obtained by applying to the sample a minimum constant load of 0.1 N. In Table I we report the mean value of the measured thermal expansion coefficient between 20–180 °C whereas in Table II we report both the storage tensile modulus and the thermal expansion coefficient evaluated at various temperatures. In our experimental conditions a good agreement has been found [27] between the dynamic storage tensile modulus and the static tensile modulus.

3.4. Residual stresses

Fragmentation measurements were performed at various temperatures by using a custom-made apparatus [15] consisting of a small tensile tester (Minimat, by Polymer Laboratories), equipped with a thermostatic chamber, and put under a polarized optical stereomicroscope (Leica-Wild M3Z). Events were recorded during the test using a Sony B/W video camera mounted on the microscope and a video-recorder. This apparatus allowed us to apply a constant strain rate (fixed at 0.008 min^{-1}) and to record the stress–strain behaviour of the sample. The strain at the fifth fibre break was evaluated by recording the applied strain which induces five breaks within a fibre probe zone 25 mm long. At least 3 samples were tested for each experimental point. To avoid errors due to the system compliance, actual sample strain was measured by monitoring, by means of the calibrated eyepiece of the microscope, the relative displacement between two transversal fiducial marks.

The mean strain at break of a single fibre in air was computed by dividing its strength, evaluated by using Equation 2, by the fibre tensile modulus (246 ± 26 GPa).

TABLE II Dynamic moduli (E'_m) and thermal expansion coefficients (α) for the epoxy and nylon-6 matrices at various temperatures

Temperature (°C)	Epoxy		Nylon-6	
	E'_m (MPa)	α (10^{-6} °K^{-1})	E'_m (MPa)	α 10^{-6} °K^{-1})
20	3000	27.9	1950	83.1
40	2830	35.8	–	–
60	2750	43.7	1020	91.9
80	2560	51.6	–	–
100	2450	59.5	780	43.1
120	2280	67.4	–	–
140	1950	75.3	500	117.2
160	50	83.2	–	–
180	–	–	250	128.4

4. Results and discussion

4.1. The strain shift effect on fragmentation

The number of fibre breaks for the epoxy–carbon microcomposite is reported in Fig. 2 for various test temperatures as a function of the applied strain. For the samples tested at high temperatures (higher than 120 °C) the whole fragmentation process has been monitored, while at lower temperature, due to the faster evolution of the fibre fragmentation, counting was limited to the first 15 breaks and therefore those data represent only the initial part of the whole standard *S*-shape curve. The shift in the data in Fig. 2 clearly reveals that residual stresses are present in the samples. A slope change occurs at temperatures higher than 120 °C (experimentally observed as a slackening of the fragmentation process), which can be explained as a consequence of the strong stiffness decrease near the matrix T_g.

The coefficient of variation (C.V.) of the strain ε^* measurements performed on three specimens was found to decrease exponentially (dotted line), as the number of fragments increased (Fig. 3). In particular the C.V. value at the first break is about 25% while the C.V. value at the fifth break lowers to about 10% which is a reasonable value for the spreading of the experimental data.

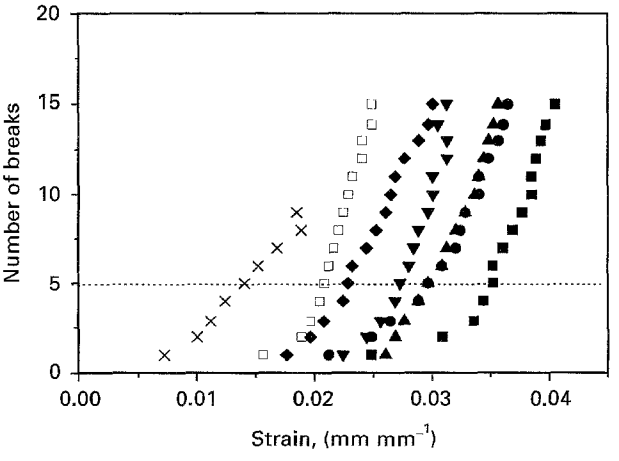

Figure 2 Number of fibre breaks versus the applied strain at various temperatures for carbon/epoxy microcomposites. The temperatures are; (■) 20 °C, (●) 40 °C, (▲) 60 °C, (▼) 80 °C, (◆) 100 °C, (□) 120 °C and (×) 160 °C.

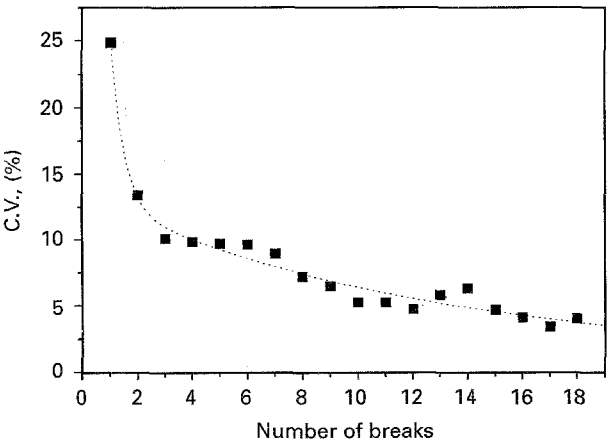

Figure 3 Coefficient of variation (C.V.) of the strain measurements as a function of the number of fibre breaks in carbon/epoxy samples.

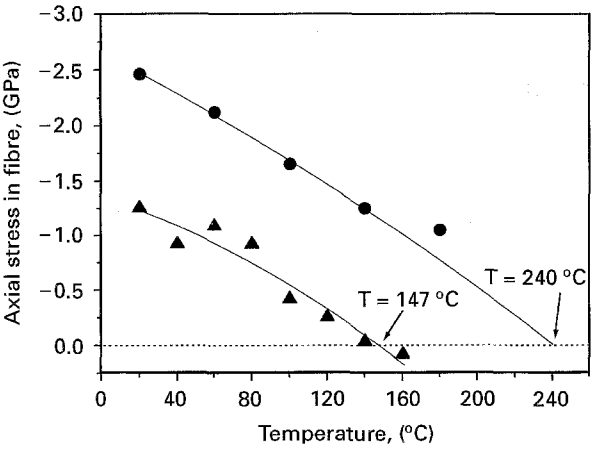

Figure 4 Effect of test temperature on the axial residual stress in the fibre measured by means of the fragmentation test for carbon/epoxy (▲) and carbon/nylon-6 microcomposites (●).

TABLE III Strain (ε*) to induce 5 fibre breaks in carbon/epoxy and in carbon/nylon-6 microcomposites as a function of test temperature

Temperature (°C)	ε* (mm mm^{-1})	
	Epoxy	Nylon-6
20	0.0220	0.0292
40	0.0200	–
60	0.0210	0.0272
80	0.0200	–
100	0.0170	0.0244
120	0.0160	–
140	0.0147	0.0220
160	0.0140	–
180	–	0.0208

4.2. Experimental measurement of the residual stresses

The amount of residual stresses in carbon/epoxy and in carbon/nylon-6 composites has been evaluated by using Equations 5 and 6, together with the data listed in Table III and the strain at break of the carbon fibre in air evaluated from SFT. For the computation of the residual stress the fibre compressive modulus (167 MPa) was used rather than the tensile one (246 MPa) because during the thermal shrinkage the fibre is gradually put under compression (see references [8] and [12]). The compressive modulus value was assumed based on the approach of Melanitis and Galiotis [28], who found, for HT PAN-based carbon fibres similar to ours, a tensile to compressive modulus ratio equal to 0.68 ± 0.07.

The computed residual stresses are reported in Fig. 4 as a function of the test temperature. As seen from Fig. 4 the residual stresses decrease in both epoxy and nylon-6-carbon composites as the test temperature increases. The slightly curved trend is due to the increment of the thermal expansion coefficient of the matrices as the temperature rises [29]. For carbon/epoxy microcomposites the interpolation curve intersects the zero stress line at 147 °C, a temperature which is between the post-curing temperature (140 °C) and the matrix T_g (152 °C). As already reported for the epoxy–carbon system [30] the stress free temperature may be chosen to be equal to the post curing temperature. It is worth noting that for the tests performed at 160 °C a slight tensile residual stress results, as expected for a positive ΔT.

In carbon/nylon-6 composites the residual stresses are larger, ranging from 2.46 GPa at 20 °C to 1.05 GPa at 180 °C. This is clearly a consequence of both the higher thermal expansion coefficient of the matrix and the wider temperature shift. The intersection between the interpolation curve and the zero stress line (Fig. 4) yields a stress free temperature equal to 240 °C. Such a value, even if slightly higher than the matrix melting temperature (226 °C), indicates that in this semicrystalline thermoplastic matrix composite the temperature at which stresses start to built is probably controlled by the crystallization process [30]. We chose the bulk matrix melting temperature as the stress free temperature for the nylon-6–carbon system. Note that the measured residual compressive stresses in the nylon-6 matrix composites cooled to room temperature should be large enough to induce some fibre breaks [8, 12]. The number of fibre breaks can be theoretically predicted [11] on the basis of the following discussion. The fibre compressive strength is assumed to follow a two parameter Weibull distribution, where the scale parameter is taken as about 50% of the tensile scale parameter [31] and the shape parameter is taken equal to the tensile shape parameter assuming the same defect population was active in both tension and compression fibre failure [8–12]. So by introducing in Equation 4 compressive scale and shape strength parameters equal to 2975 MPa and 4.8 respectively we obtain that, due to compressive thermal stresses, the fibre should break in fragments 12.5 mm long, which means that on average 1 break should be present in the sample prior to fragmentation test. Our experimental observations indeed revealed an average occurrence of about 1 compressive break in the carbon/nylon-6 samples. Note that if the tensile modulus is considered the residual stress should reach a value of 3.44 GPa, consequently inducing about 7 fibre breaks. These considerations further support the use of the compressive modulus rather than the tensile one to estimate the residual stresses.

TABLE IV Fibre residual stresses both experimentally measured (fragmentation test) and evaluated by means of the Tsai–Hahn theoretical model (theory) for the epoxy and nylon-6 matrix microcomposites

Temperature (°C)	Thermal stress (GPa)			
	Epoxy		Nylon-6	
	fragmentation test	theory	fragmentation test	theory
20	− 1.252	− 1.065	− 2.461	− 3.623
40	− 0.919	− 0.885	–	− 3.274
60	− 1.093	− 0.708	− 2.124	− 2.924
80	− 0.919	− 0.531	–	− 2.566
100	− 0.418	− 0.354	− 1.653	− 2.208
120	− 0.251	− 0.177	–	− 1.860
140	− 0.344	0.000	− 1.252	− 1.512
160	0.835	0.261	–	− 1.162
180	–	–	− 1.048	− 0.812

TABLE V Effect of the fibre volume fraction (ϕ) on the thermal stresses evaluated by means of the Tsai–Hahn theoretical model for both the epoxy and nylon-6 matrix microcomposites. Columns (a) or (b) correspond to the fibre volume fractions computed as described in Fig. 5a, b respectively

Temperature (°C)	Thermal stresses (GPa)			
	Epoxy		Nylon-6	
	(a) $\phi = 9.60 \times 10^{-6}$	(b) $\phi = 4.90 \times 10^{-5}$	(a) $\phi = 4.00 \times 10^{-5}$	(b) $\phi = 1.33 \times 10^{-3}$
20	− 1.065	− 1.064	− 3.623	− 3.262
40	− 0.885	− 0.883	− 3.274	− 2.940
60	− 0.708	− 0.706	− 2.924	− 2.618
80	− 0.531	− 0.530	− 2.566	− 2.305
100	− 0.354	− 0.353	− 2.208	− 1.992
120	− 0.177	− 0.177	− 1.860	− 1.676
140	0.000	0.000	− 1.512	− 1.360
160	0.261	0.260	− 1.162	− 1.046
180	–	–	− 0.812	− 0.731

4.3. Comparison with theoretical model

The residual stresses measured experimentally by the fragmentation test have been compared with the thermal stresses evaluated by means of the Tsai–Hahn model (Equation 7) using the data reported in Table I. The stress free temperatures, according to the above observations, were 140 °C for carbon/epoxy samples and 226 °C for carbon/nylon-6 samples. The fibre volume fractions were 9.60×10^{-6} for epoxy resin microcomposites and 4.00×10^{-5} for nylon-6 matrix microcomposites. The results are listed in Table IV. For carbon/epoxy composites there is a satisfactory fit between the theoretical and the experimental values of the thermal stresses whereas in carbon/nylon-6 composites the theoretically estimated values are higher than the experimental ones. Such higher values should induce more compressive fragmentation than observed, but the data in Table IV were obtained by considering the whole matrix cross-sectional area in the fibre volume fraction computation, and no temperature dependent properties for the matrix.

The effect of the fibre volume fraction on residual thermal stresses can be understood from the data listed in Table V, where thermal stresses are evaluated assuming two different calculations of the fibre volume fractions. In the first case, all the sample matrix is considered for the fibre volume fraction calculation, while in the second case, only the matrix cylinder surrounding the fibre with a diameter equal to the sample thickness is considered (see Fig. 5). From Table V it results that in nylon-6 matrix samples the fibre volume fraction effect is not negligible whereas for the epoxy resin matrix samples no appreciable variation is obtained. At this point one may ask: what is the correct fibre volume fraction to include in the computation? Concerning this two observations must be reported: (i) a cylindrical field for the thermal stresses seems to be more reasonable than a "flattened" one which extends in a direction (width) almost two orders of magnitude larger than in the order direction (thickness); (ii) the fibre volume fraction corresponding to Fig. 5a should induce larger compressive stresses in the sample and a more extensive fibre fragmentation prior to testing. This is not experimentally observed and therefore, based on the above considerations, the fibre volume fraction which corresponds to Fig. 5b should better describe the microcomposite behaviour. Accordingly, we take a volume fraction of 4.90×10^{-5} for epoxy resin samples and 1.33×10^{-3} for nylon 6 matrix samples.

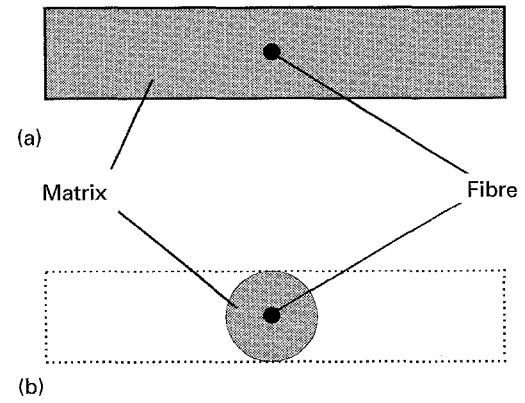

Figure 5 Schematic illustration of different fibre volume fraction computations: (a) one single fibre embedded in matrix whose area is equal to the sample cross-section, (b) one single fibre embedded in a matrix cylinder whose radius is equal to the sample thickness.

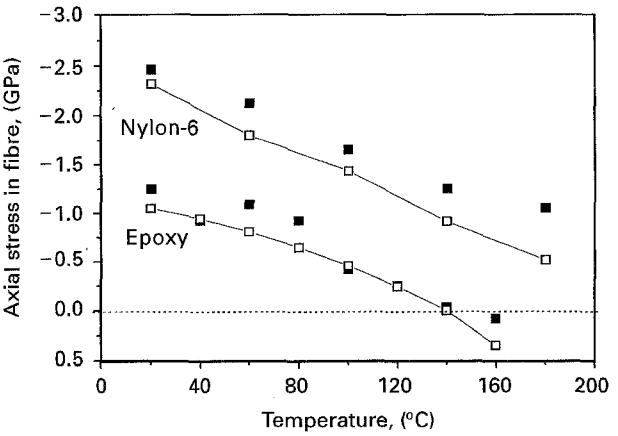

Figure 6 Effect of test temperature on the axial residual stress in the fibre by the fragmentation test (■) and the Tsai-Hahn theoretical model (□) for carbon/epoxy and carbon/nylon-6 microcomposites.

TABLE VI Effect of temperature on the thermal stresses evaluated by means of the Tsai–Hahn theoretical model. The results of column (I) were obtained by considering temperature independent properties, while results of column (II) were obtained taking in to account the effect of temperature on matrix properties

Temperature (°C)	Thermal stresses (GPa) Epoxy		Nylon-6	
	(I)	(II)	(I)	(II)
20	− 1.064	− 1.049	− 3.262	− 2.313
40	− 0.883	− 0.940	− 2.940	–
60	− 0.706	− 0.804	− 2.618	− 1.799
80	− 0.530	− 0.642	− 2.305	–
100	− 0.353	− 0.454	− 1.992	− 1.432
120	− 0.177	− 0.241	− 1.676	–
140	0.000	0.000	− 1.360	− 0.912
160	0.260	0.389	− 1.046	–
180	–	–	− 0.731	− 0.511

To include the thermal dependence of the matrix properties, the Tai–Hahn equation was integrated by standard numerical procedures using Young's moduli and the thermal expansion coefficients of the matrices, measured at various temperatures. The resulting thermal stresses are listed in Table VI (columns II), where the previously obtained data (columns I) are also reported for comparison. In carbon/epoxy composites the thermal stresses obtained using matrix temperature dependent properties are quite similar to the values obtained with constant matrix properties, although at high temperature they are slightly larger. This results from the fact that near T_{ref} the coefficient of thermal expansion is larger than the mean value considered for the whole temperature range. The temperature dependence of matrix properties has a stronger effect on the thermal stresses in the case of carbon/nylon-6 composites. This is mainly due to the decrease of Young's modulus of nylon-6 above T_g (53.5 °C). This effect is not so important in epoxy samples due to the high modulus values of epoxy up to its T_g.

In Fig. 6 we compare the experimental results with the theoretical data presented in Table VI (column II). The agreement is quite good both for carbon/epoxy and carbon/nylon-6 microcomposites thus confirming the reliability of the proposed experimental technique. Fig. 6 reveals that in nylon-6 matrix composites the data are slightly higher than the predicted stresses, and the discrepancy seems to increase as the temperature increases. That behaviour is probably due to the increasing sample compliance as the temperature rises: indeed the actual fibre strain is then probably smaller than the sample strain and therefore leads to an overestimation of the residual stresses. Further investigation of that issue is part of a current work in progress.

5. Conclusions

Axial residual stresses in thermosetting and thermoplastic microcomposites have been measured by an original technique based on the fragmentation test. The experimental results have been compared with data obtained from the Tsai–Hahn theoretical model. In general a good agreement was found, but a better comparison is obtained if the temperature dependence of Young's modulus and thermal expansion coefficient of the matrix are accounted for and if the appropriate volume fraction is chosen.

It was shown that for the carbon fibre microcomposites the fibre compressive properties must be accounted for in evaluating the thermal stresses. For the composite thermosetting matrix under investigation, tests conducted at various temperatures have shown that the residual fibre longitudinal stress decreased as the temperature increased, and that this stress disappeared at a temperature that approximately corresponds to the post-curing temperature of the matrix. In thermoplastic matrix microcomposites the fibre axial residual stress was large enough to induce compressive fibre breaks, as theoretically expected. This stress also decreased for increasing temperatures, up to a stress-free point corresponding approximately to the melting temperature of the matrix.

Acknowledgements

This work was partially supported by C.N.R. Comitato Tecnologico, Rome, Italy.

References

1. B. D. AGARWAL and L. J. BROUTMAN, "Analysis and performance of fibre composites" (John Wiley & Sons, New York, 1992).
2. H. T. HAHN, *J. Compos. Mater.* **10** (1976) 226.
3. H. T. HAHN and N. J. PAGANO, *ibid* **9** (1975) 91.
4. R. B. PIPES, J. R. VINSON and T. W. CHOW, *ibid* **10** (1976) 129.
5. G. JERONIMIDIS and A. T. PARKYN, *ibid* **22** (1988) 401.
6. J. A. NAIRN, *Polym. Compos.* **6** (1985) 123.
7. L. DILANDRO and M. PEGORARO, in Proceedings of Interfacial Phenomena in Composites Materials '91, Leuven, September 1991, edited by I. Verpoest and F. Jones (Butterworths, London, 1991) p. 93.
8. H. D. WAGNER, *J. Adhesion* **52** (1995) 131.
9. H. D. WAGNER, C. MIGLIARESI, A. H. GILBERT and G. MAROM, *J. Mater. Sci.* **27** (1992) 4175.
10. S. INCARDONA, C. MIGLIARESI, H. D. WAGNER, A. H. GILBERT and G. MAROM, *Comp. Sci. & Techn.* **47** (1993) 43.
11. H. D. WAGNER, J. WOOD and G. MAROM, *Adv. Comp. Letters* **2** (1993) 173.
12. H. D. WAGNER, *Comp. Interfaces* **2** (5) (1995) 321.
13. G. ZHANG and R. T. LATOUR, *Composites Science and Technology* **51** (1994) 95.
14. M. R. PIGGOTT, *ibid* **30** (1987) 295.
15. M. DETASSIS, A. PEGORETTI and C. MIGLIARESI, *ibid* **53** (1995) 39.
16. W. A. FRASER, F. H. ANCKER, and A. T. DIBENEDETTO, in Proceedings of the 30th Ann. Techn. Conf. SPI Reinf. Plastics Division-Composite Inst., Washington D.C. USA, 22-A (1975) p. 1.
17. A. KELLY and W. R. TYSON, *J. Mech. Phys. Solids* **13** (1965) 329.
18. T. OHSAWA, A. NAKAYAMA, M. MIWA and A. HASEWAGA, *J. Appl. Polym. Sci.* **22** (1978) 3203.
19. W. WEIBULL, *J. Appl. Mech.* **18** (1951) 293.
20. EL. M. ASLOUN, J. B. DONNET, G. GUILPAIN, M. NARDIN and J. SCHULTZ, *J. Mater. Sci.* **24** (1989) 3504.
21. B. YAVIN, H. E. GALLIS, J. SCHERF, A. EITAN and H. D. WAGNER, *Polym. Compos.* **12** (1991) 436.
22. C. A. BAILLIE and M. G. BADER, *Composites* **25** (1994) 401.
23. J. SCHERF and H. D. WAGNER, *Polym. Eng. and Sci.* **32** (1992) 298.
24. P. VAUTEY, M. C. MERIENNE, C. COTTENOT, and J. P. FAVRE, in Proceedings of Interfacial Phenomena in Composites Materials '89, Sheffield, September 1989, edited by F. Jones (Butterworths, London, 1989) p. 53.
25. M. C. WATERBURY and L. T. DRZAL, *J. Compos. Techn. & Research* **13** (1991) 22.
26. S. W. TSAI and H. T. HAHN, "Introduction to Composite Materials", (Technomic Publ. Co., Inc. Westport, CT, 1980) p. 404.
27. A. PEGORETTI, M. DETASSIS, H. D. WAGNER and C. MIGLIARESI, *Composites* submitted.
28. N. MELANITIS and C. GALIOTIS, *J. Mater. Sci.* **25** (1990) 5081.
29. F. MARK, N. M. BIKALES, C. G. OVENBERGER, G. MENGES and J. I. KRONSCHWITZ, "Encyclopedia of Polymer Science and Engineering" (John Wiley & Sons, New York, 1989) Vol 16, p. 745.
30. J. A. NAIRN and P. ZOLLER, *J. Mater. Sci.* **20** (1985) 355.
31. T. OHSAWA, M. MIWA, M. KAWADE and E. THUSHIMA, *J. Appl. Polym. Sci.* **39** (1990) 1733.

Received 17 February 1995
and accepted 20 November 1995